Nishii, Ho, Chou, Gabotti, Wang, Spada & Möller 2014

GA2 and GA20-oxidase expressions are associated with the meristem position in Streptocarpus rexii (Gesneriaceae).

Plant Growth Regul 72:123–140.

REFNO: 3992

KEYWORDS:

Basal meristem, Gibberellin20-oxidase,

Gibberellin2-oxidase, Gibberellins, Macrocotyledon,

Streptocarpus

Plant Growth Regul (2014) 72:123–140
DOI 10.1007/s10725-013-9844-1

ORIGINAL PAPER

GA2 and *GA20-oxidase* expressions are associated with the meristem position in *Streptocarpus rexii* (Gesneriaceae)

Kanae Nishii · Meng-Jung Ho · Yen-Wei Chou · Damiano Gabotti · Chun-Neng Wang · Alberto Spada · Michael Möller

Received: 1 March 2013 / Accepted: 24 September 2013 / Published online: 6 October 2013

Abstract We examined genes involved in the regulatory pathway of gibberellin (GA) in meristems of *Streptocarpus rexii*. The plants do not possess a typical shoot apical meristem (SAM) and form unique meristems: the basal meristem extends the lamina area of one cotyledon to produce anisocotylous seedlings; the groove meristem forms new leaves at the base of the macrocotyledon. Exogenous application of GA significantly suppresses the basal meristem activity in developing cotyledons and the seedlings remain isocotyl. To examine the role of endogenous GA on these meristems in vivo, we isolated homologs of *GA2-oxidase* responsible for degrading active GAs (*SrGA2ox*), and *GA20-oxidase* regulating the rate limiting step of active GA synthesis (*SrGA20ox*). During embryogenesis, while first partly overlapping, the expression of *SrGA2ox* and *SrGA20ox* became more differentiated and mutually exclusive, ending with *SrGA2ox* being expressed solely in the adaxial–proximal domain of the embryo in regions with meristem activity, whereas *SrGA20ox* was restricted to the fork between the two cotyledons. The latter may be responsible for suppressing the formation of an embryonic SAM in *S. rexii*. In developing seedlings, *SrGA2ox* expression also followed the centers of meristem activity, where *SrGA20ox* expression was excluded. Our results suggest that low levels of GA are required in *S. rexii* meristems for their establishment and maintenance. Thus, the meristems in *S. rexii* share similar regulatory pathways suggested for the SAM in model plants, but that in *S. rexii* evolutionary modifications involving a lateral transfer of function, from shoot to leaves, is implicated in attaining the unusual morphology of the plants.

Keywords Basal meristem · *Gibberellin20-oxidase* · *Gibberellin2-oxidase* · Gibberellins · Macrocotyledon · *Streptocarpus*

Kanae Nishii and Meng-Jung Ho have equally contributed to this work.

Electronic supplementary material The online version of this article (doi:10.1007/s10725-013-9844-1) contains supplementary material, which is available to authorized users.

K. Nishii (✉) · M.-J. Ho · Y.-W. Chou · C.-N. Wang (✉)
Department of Life Science, Institute of Ecology and Evolutionary Biology, National Taiwan University, No. 1, Sec. 4, Roosevelt Road, Taipei 10617, Taiwan
e-mail: kanaenishii@ntu.edu.tw

C.-N. Wang
e-mail: leafy@ntu.edu.tw

K. Nishii · M. Möller
Royal Botanic Garden Edinburgh, 20A Inverleith Row, Edinburgh EH3 5LR, Scotland, UK

D. Gabotti · A. Spada (✉)
Milan University Dipartimento Scienze Agrarie e Ambientali Territorio e Agroenergia, Università degli Studi di Milano, Via Celoria 2, 20133 Milan, Italy
e-mail: alberto.spada@unimi.it

Introduction

One of the key issues in evolutionary developmental biology is to shed light on the mechanisms that underlie plant architecture. The shoot apical meristem (SAM) is an indeterminate structure that gives rise to the aerial plant organs. In the model plant *Arabidopsis thaliana,* the SAM is established between the cotyledons during embryogenesis (Jürgens 2001). After germination, the SAM repetitively develops leaf–stem units, called phytomers, to form shoots (Steeves and Sussex 1989).

Recent studies revealed that class 1 *knotted-like* (*KNOX1*) homeobox genes play important roles in the maintenance of indeterminacy of cells in the SAM (Hake et al. 2004). Plant hormones, such as cytokinin (CK) or gibberellin (GA), are important regulators for *KNOX1* genes. GA, in particular, is involved in organ determination (Hay et al. 2002; Jasinski et al. 2005). It is synthesized in determinate organ primordia to maintain high levels of GA there, and is excluded from the SAM (Veit 2004). The transcriptional regulation of oxidases relating to GA synthesis and degradation is important in this process. For instance, *GA20-oxidase* and *GA2-oxidase* control the GA biosynthesis and degradation respectively, and are responsible for regulating localized GA concentrations in the SAM and organ primordia (Sakamoto et al. 2001a, b; Hay et al. 2002; Jasinski et al. 2005; Bolduc and Hake 2009). GA20-oxidase is a 2-oxoglutarate-dependent dioxygenase and responsible for 2-beta-hydroxylation and controls rate-limiting steps in GA biosynthesis. On the other hand, GA2-oxidase deactivates active GAs via 2-oxidation of 2-beta-hydroxylated GAs (Olszewski et al. 2002).

In the shoot apex of *A. thaliana* and rice, *GA20-oxidase* is expressed in leaf primordia or developing leaves (Sakamoto et al. 2001a; Hay et al. 2002), whereas *GA2-oxidase* is expressed along the edges of the SAM and prevents the GA import into the SAM (Sakamoto et al. 2001b; Jasinski et al. 2005).

Although the SAM is a common feature in most plants, in acaulescent species of the genus *Streptocarpus* (Gesneriaceae), such as *S. rexii*, a SAM is not formed (Jong 1970; Mantegazza et al. 2007; Nishii and Nagata 2007), and they do not form typical phytomers (Jong and Burtt 1975). Instead, acaulescent *Streptocarpus* possess a series of lamina–petiolode constructs, termed phyllomorphs, with the subtending petiolode retaining features of petiole and stem (Jong and Burtt 1975; Imaichi et al. 2000; Mantegazza et al. 2007). The meristem activity in phyllomorphs is unique among plants and includes a nexus of three meristems: the basal meristem in the proximal region of the lamina continuously extending the lamina, the petiolode meristem responsible for its elongation, and the groove meristem located on the petiolode near the base of the lamina forming new phyllomorph primordia or inflorescences (Jong and Burtt 1975; Imaichi et al. 2000; Nishii et al. 2004; Nishii and Nagata 2007). The first phyllomorph to develop in *Streptocarpus* is formed by one cotyledon (the macrocotyledon) to result in anisocotylous seedlings while the other cotyledon (the microcotyledon) withers away (Fig. 1; Online Resource 1; Jong 1970; Imaichi et al. 2000; Mantegazza et al. 2007). Thus, rosulate species of *Streptocarpus*, such as *S. rexii*, possess a cotyledonary phyllomorph with additional phyllomorphs formed by the groove meristem (Online Resource 1; Jong 1970; Jong and Burtt 1975).

Previous studies suggested that genetic and physiological pathways are involved in the unique phyllomorph morphogenesis of *Streptocarpus*. *KNOX1* genes were isolated and characterized in *S. rexii* (Harrison et al. 2005; Nishii et al. 2010), and *SrSTM1* was found expressed during embryogenesis in the cotyledons but not in between the cotyledons where ordinary plants form a SAM. After germination, *SrSTM1* expression was initially observed in both cotyledons, but later only in the macrocotyledon coinciding with the area of cell division of the basal meristem (Mantegazza et al. 2007, Nishii et al. 2010). *SrBP* was studied in post-germination seedlings only and found to follow the *SrSTM1* pattern (Nishii et al. 2010). This suggests some conserved functions of *KNOX1* genes in the meristem formation and functioning between model plants and *S. rexii*, though with a modified spatial–temporal regulation in *Streptocarpus.*

Exogenous applications of plant hormones affect the anisocotylous development in *Streptocarpus* (Rosenblum and Basile 1984; Nishii et al. 2004; Mantegazza et al. 2009; Nishii et al. 2012). 6-benzylaminopurine (BAP) resulted in the formation of two macrocotyledons (Mantegazza et al. 2009; Nishii et al. 2004, 2012), while, in contrast, GA_3 prevented macrocotyledon growth and resulted in two microcotyledon-like cotyledons (Rosenblum and Basile 1984; Mantegazza et al. 2009; Nishii et al. 2004, 2012). In both cases, the groove meristem was relocated to the fork between the equally sized cotyledons and leaf-like structures formed from this meristem, along with a delocalization of *SrSTM* expression (Mantegazza et al. 2009). This suggests that GA and CK play major roles in the meristem establishment, development and maintenance in *Streptocarpus*. Together with the conservation of *KNOX1* gene function, the unorthodox body plan of *S. rexii* may thus not be due to novel genes but may be caused by a variation in expression of conserved genes (Lavoie et al. 2010).

To address this possibility, and since plant hormones are involved in the establishment of anisocotyly, in this study we directly tested the involvement of GA metabolic genes in the formation and regulation of meristems in *S. rexii*. We therefore isolated *S. rexii* homologs of the GA degradation gene *GA2-oxidase* and the GA biosynthesis gene *GA20-oxidase,* and studied their expression patterns during embryogenesis and germination until the establishment of seedling anisocotyly in relation to the meristematic activity in seedling tissues and exogenous GA and CK applications.

Materials and methods

Plant materials

Materials for study came from *S. rexii* plants (original seed collection from Tsitsikamma, Cape Province, SA, Royal

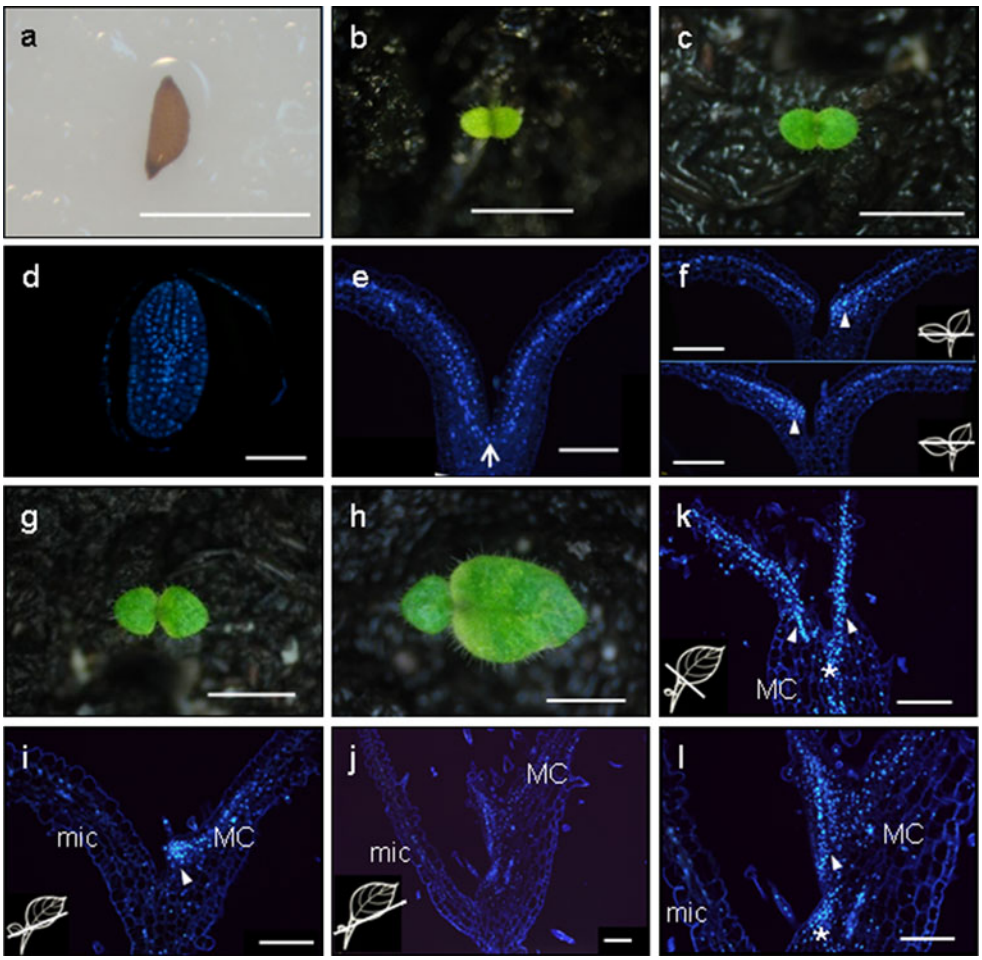

Fig. 1 Seedling development in *S. rexii*. **a**–**c**, **g**, **h** Morphology of seed and developing seedling. **d**–**f**, **i**–**l** DAPI staining of nuclei in sections of seed and developing seedlings. **d**–**f**, **i**, **j**, **l** Longitudinal section (LS). **k** Transverse section (TS). **a**, **d** Imbibed seed. **b**, **e** Seedling with fully unfolded cotyledons representing 'day 1 after cotyledon unfolding' (1 DCU). **e** A SAM is not observed between cotyledons (*arrow*). **c**, **f** 3 DCU; isocotylous stage. **f** Serial LS sections of a seedling. Both cotyledons (*upper* and *lower columns*) show basal meristem activity (*arrowheads*). **g**, **i** 7 DCU; beginning of anisocotylous stage. One cotyledon become larger than the other. **i** The macrocotyledon (MC) shows basal meristem activity (*arrowhead*). **h**, **j**, **k**, **l** 21 DCU; anisocotylous stage. The basal meristem (*arrowheads*) and the groove meristem (*asterisks*) have been established. MC: macrocotyledon, mic: microcotyledon. *Bars* 1 mm (**a**–**c**, **g**, **h**), 100 μm (**d**–**f**, **i**–**l**)

Botanic Garden Edinburgh, RBGE, accession number 20030814) cultivated at continuous 23 °C under 16 h light (54 μmol m^{-2} $s^{-}1$) and 8 h darkness, and a relative humidity of 80 %. Mature plants were fertilized with HYPONeX #4 (N–P–K = 6.5–6–19; 1:1,000 w/v in tap water; HYPONeX Corporation, Ohio, USA) every 2 weeks. For studies on developing embryos, fruits were collected in weekly intervals after artificial pollination until seed maturity. Seed for germination experiments also came from self-pollinated flowers. They were sown in soil or filter paper in 9 cm Petri dishes and germinated under the same conditions as the plants above.

Morphological and anatomical analyses

The developing seedling morphology was observed under a SteREO stereomicroscope (Zeiss, Oberkochen, Germany), and images taken with an AxioCam Icc3 camera (Zeiss). The seedlings were fixed in FAA (3.7 % formaldehyde, 5 % acetic acid, 50 % ethanol in water) at different stages of development up to day 21 of cotyledon unfolding (DCU), dehydrated in an ethanol series, then transferred to xylene and embedded in paraffin for sectioning. The paraffin sections were cut to 10 μm thickness and treated with xylene for de-waxing, then hydrated in an ethanol series (Mantegazza et al. 2007) and stained with 1 μg/ml 4′,6-diamidino-2-phenylindole (DAPI). DAPI binds specifically to DNA allowing the visualization of the nucleus in cells under UV. It is reasoned that meristematic cells have a high ratio of nuclei thus characterizing meristematic regions (Cutler et al. 2007). Stained sections were observed under a fluorescence microscope BX 51 (Olympus, Tokyo, Japan) using a UV-excitation filter.

Images were taken with a CCD camera, DP 71 (Olympus) for further analysis.

Exogenous GA_3 treatment of seedlings

GA_3 (Sigma, St. Lois, USA) was diluted in dimethyl sulfoxide (DMSO) (GA_3 : DMSO, 1:1,000). This stock solution was further diluted with distilled water to 3×10^{-5} M GA_3 final concentration, and once directly added to the soil in Parafilm-sealed Petri dishes when sowing. An equivalent amount of DMSO was added to water and applied to the soil in controls. The seedling morphology at different developmental stages was examined at 1 DCU, 5 DCU (still isocotyly), and 10 DCU (anisocotyly). For this, the seedlings were fixed in Et-OH : acetic acid (4:1), cleared in chloral hydrate (Nishii et al. 2004) and digital images taken with a CCD camera, DP 71 (Olympus) mounted on a brightfield microscope BX51 (Olympus). On these digital images the cotyledon area was analyzed in ImageJ v1.44x (Schneider et al. 2012), and the number of subepidermal cells along the longitudinal axis of the cotyledons and the number of lateral veins were counted. The number of lateral veins was found to be a good character for the identification of the macrocotyledon (Nishii et al. 2004; Mantegazza et al. 2009).

The seedlings were also stained with Aniline Blue (Sigma) as previously described (Kuwabara and Nagata 2006). Aniline Blue staining detects the septum walls of newly divided cells (Hayashi et al. 1986; Nishii et al. 2004). For this, seedlings were fixed in ethanol : acetic acid (4:1; v/v), hydrated in an ethanol series, then transferred to a phosphate buffer and stained in a 0.02 % Aniline Blue solution. The epidermal and subepidermal cells of stained samples were observed from the adaxial side of the cotyledons under a fluorescence microscope BX51 (Olympus). To examine the effects of GA_3 on the meristematic activity, the number of fluorescing cell planes in the epidermal and subepidermal cells per cotyledon was counted at 1, 5, and 10 DCU. We also determined the position of Aniline Blue stained cell walls in ImageJ v1.44x. XY coordinate data of the cotyledon contour, and graphically illustrated these in Microsoft Office Excel (Microsoft, Redmond, USA).

Isolation of *GA2-oxidase* and *GA20-oxidase* homolog sequences

Degenerate primers were designed based on known *GA2-oxidase* sequences in other species, such as *A. thaliana*, *Ipomoea nil* and *Populus trichocarpa*. The degenerate primers, GA20-LPWK-F (5′-TCT TCT AAG CTG CCT TGG AAR GAR AC-3′), and GA20-QKHY-R (5′-AGT ATT CAT ATC AGC TCT ATA RTG YTT YTG-3′) were designed in CODEHOP (Staheli et al. 2011) and used in polymerase chain reaction (PCR) amplifications on cDNA of whole plants of *S. rexii* using standard PCR conditions. 3′ RACE PCRs were carried out with primer GA2-ox1-FRVN (5′-TCC GGG TGA ATC ACT ACC CTC CAT GCC CAG-3′) to obtain the 3′ region. Inverse PCRs were carried out to obtain whole sequences according to Ochman et al. (1988). 1 μg of genomic DNA was digested by *EcoRI* and ligated with T4 DNA ligase. The circularized DNA was used as templates for PCR amplifications with the primers GA2-ox1-KVGP (5′-AAG CAG AAA GTT GGT CCC CC-3′) and GA2-ox1-WLEY (5′-GTA TTC AAG CCA GCC GAC GT-3′).

To isolate *GA20-oxidase* gene homologs from *S. rexii*, the degenerate primers GA20-DLGG-F (5′-GAC TTA RGR GGY TTY CTT TCT GG-3′), and GA20-HYRA-R (5′-AGR GTG TTC ATR TCA GCT CTR TAA TG) were designed from published *GA20-oxidase* sequences of *Nicotiana tabacum*, *Solanum lycopersicum* and *Nerium oleander*. After partial sequences were obtained, 5′ and 3′ RACE PCRs were carried out (Mantegazza et al. 2007) to isolate the full open reading frame of the *GA20-oxidase* homologs.

The homology of the isolated genes to characterized genes from model plants was tested on deduced amino acid sequences of the obtained nucleotide sequences of *GA2-oxidase* and *GA20-oxidase*, aligned in BioEdit version 7.1.3. (Hall, Ibis Biosciences, Carlsbad, CA, USA), respectively. Neighbor-joining trees based on the deduced amino acid sequences of conserved regions for *GA2-oxidase* and *GA20-oxidase* genes were constructed in PAUP* version 4.0b10 (Swofford 2002). Bootstrap analyses for each tree were performed with 10,000 replicates. The nucleotide and deduced amino acid similarity between the obtained sequences and reference sequences was calculated in SIAS (Sequence Identity and Similarities; http://imed.med.ucm.es/Tools/sias.html).

Real-time PCR gene expression analyses

GA2- and *GA20-oxidase* mRNA transcription was assessed by real-time PCR. Total RNA was extracted using Trizol (Invitrogen, Carlsbad, CA, USA) and cDNA was synthesized with oligo dT primers or gene specific primers with Superscript III reverse transcriptase (Invitrogen) following the manufacturer's protocol. Gene specific primer pairs spanning intron regions were used for real-time PCR amplification; for *SrGA2ox*, GA2ox-WLEY-F (5′-ACG TCG GCT GGC TTG AAT AC-3′) and GA2ox-VKKM-R (5′-CCA TCT TCT TCA CCG CCG AT-3′), for *SrGA20ox*, GA20ox-AHKD-F (5′-GCG CAC AAG GAC TCA TCA CA-3′) and GA20ox-AMSE-R (5′-AGT TCG CTC ATC GCA CTA CA-3′). *18S rRNA* was amplified as internal

control using primers Q18SF (5′-TGA CGG AGA ATT AGG GTT CGA-3′) and Q18SR (5′-GGA TGT GGT AGC CGT TTC TCA-3′). Real-time PCR was carried out with the KAPA SYBR FAST qPCR kit (KAPA Biosystems, Woburn, MA, USA), using a Bio-Rad CFX real-time PCR machine (Bio-Rad, Hercules, CA, USA). The melting curve was analyzed for each experiment individually for each primer set. The efficiency of the primer pairs and the obtained threshold cycle (Ct) values were analyzed in REST (Pfaffl et al. 2002). All experiments were conducted in triplicates. Relative gene expression levels were calculated using *18S rRNA* as reference and a hypothesis test [*P*(*H1*)] performed in REST.

Relative gene expression levels were examined in untreated plants: in cotyledons of isocotylous seedlings at 3–5 DCU, in the macrocotyledon and the microcotyledon at 40 DCU against an entire seedling at the same developmental stage, and in a newly formed phyllomorph in mature plants against an entire plant.

In situ hybridization

mRNA in situ hybridization was carried out following methods employed in Nishii et al. (2010). To synthesize gene specific RNA probes, the partial sequence of *SrGA2ox* (positions in *SrGA2ox* nucleotide sequence 839-1123, including the 3′UTR region), *Sr20ox* (positions in *SrGA20ox* nucleotide sequence 808-1059) were cloned into the pGEM-T easy vector system (Promega, Fitchburg, WI, USA) respectively. These plasmids were digested with *SpeI* (Thermo Fisher Scientific Inc., Waltham, MA, USA). Digoxigenin (DIG)-labeled RNA was synthesized with DIG-dNTP (Roche Diagnostics GmbH, Basel, Switzerland) and T7 RNA polymerase. The plant material was fixed in 4 % paraformaldehyde and processed for paraffin embedding and sectioning as described above. The sections were hybridized with RNA probes and hybridization detected by Anti-DIG-AP (Roche Diagnostics GmbH) with NBT/BCIP as substrate. Hybridization was visible as purple to blue signals. The sections were observed under a BX51 (Olympus) microscope under bright field, or dark field for improved contrast. Sense transcripts of each gene were used for negative controls.

The definition of developmental stages of embryogenesis in *S. rexii* followed previous studies (Mantegazza et al. 2007, 2009, Tononi et al. 2010). In the present study, we examined the embryo at the late globular stage to maturity, focusing on the development of the cotyledon primordia. At the late globular stage to early heart stage, the cotyledon primordia are initiating. During the heart stage and the linear cotyledon stage, the cotyledons develop and form the mature seed (see Fig. 2 in Mantegazza et al. 2007). The linear cotyledon stage is equivalent to the torpedo stage in *A. thaliana* (Park and Harada 2008), though in *S. rexii*, cotyledons remain linear in the mature embryo.

The effects of hormone treatments on *SrGA2ox*/*SrGA20ox* expression levels

To examine the effects of GA or CK treatments on gene expressions, seedlings at 50 DCU with a macrocotyledon length of 1.5 cm, were transferred to filter paper and cultured for 10 days with or without 3×10^{-5} M GA_3 or 10^{-5} M BAP. The expression levels of *SrGA2ox* and *SrGA20ox* were analyzed by real-time PCR as described above.

Relative expression levels were determined in macrocotyledons (plus petiolode) in seedlings treated with GA or CK at 50 DCU against levels in macrocotyledons of control samples cultured without hormones. *18SrRNA* was used as internal standard, and a hypothesis test [*P(H1)*] performed in REST. All experiments were conducted in triplicates and two biological repeats were carried out.

Results

Anisocotylous seedling development

Seeds (Fig. 1a, d) started germinating 13–15 days after sowing and at day 1 of cotyledon unfolding (DCU) a plumula between the two cotyledons was not detectable (Fig. 1b, e). The cotyledons were still equal in size at 3 DCU (Fig. 1c). At this stage, DAPI staining showed a high concentration of nuclei in the proximal region of both cotyledons but not in the fork between the cotyledons (Fig. 1f), confirming the presence of meristematic cells in both cotyledons (the basal meristem initials) and the absence of an embryonic SAM. At 7 DCU, one cotyledon had become slightly larger than the other, and DAPI staining had shifted to the proximal region of the larger cotyledon indicating the location of the established basal meristem that extended the lamina (Fig. 1g, i). Thus, anisocotylous growth starts from about 7 DCU in *S. rexii* under our growth conditions. The macrocotyledon continued to develop into a cotyledonary phyllomorph, possessing a basal meristem and a groove meristem (Fig. 1h–l, Online Resource 1).

Effects of exogenous application of gibberellin

The GA_3 treatment affected the normal anisocotyly development in *S. rexii* (Fig. 2; Table 1). While the control seedlings showed typical anisocotyly (Fig. 2a), seedlings treated with 3×10^{-5} M GA_3 remained isocotylous (Fig. 2b, c) and formed a new phyllomorph between the two

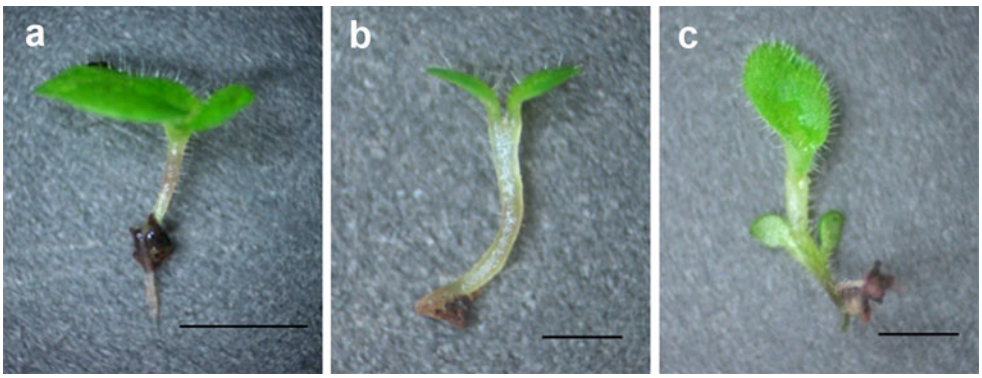

Fig. 2 Morphology of untreated and GA_3 treated *S. rexii* seedlings. **a** A control seedling 30 DCU showing anisocotyly. **b**, **c** Gibberellin (3×10^{-5} M GA_3) treated seedlings. **b** 15 DCU. **c** 30 DCU. The macrocotyledon formation is inhibited by GA_3 (**b**), and a new phyllomorph initiated between the cotyledons (**c**). *Bars* 1 mm (**a**, **c**), 0.5 mm (**b**)

Table 1 The effects of GA_3 treatment on cotyledon development in *S. rexii* seedlings

	1 DAU		5 DAU		10 DAU	
	Larger co.	Smaller co.	Larger co.	Smaller co.	Larger co.	Smaller co.
Control						
Area of cotyledon (mm^2)	0.34 ± 0.05	0.31 ± 0.04	0.54 ± 0.03	0.47 ± 0.02	1.75 ± 0.16	1.01 ± 0.10
No. of cells	37.0 ± 2.0	34.0 ± 3.0	53.8 ± 2.6	40.0 ± 3.0	81.6 ± 2.8	43.4 ± 3.7
No. of AB stained cell walls	12.4 ± 1.4	12.6 ± 2.5	13.2 ± 3.1	2.4 ± 0.6	21.6 ± 3.0	0.8 ± 0.5
No. of lateral veins	0 ± 0	0 ± 0	0 ± 0	0 ± 0	2.4 ± 0.4	0 ± 0
GA_3 treated						
Area of cotyledon (mm^2)	0.24 ± 0.01	0.22 ± 0.01	0.48 ± 0.03	0.43 ± 0.03	0.94 ± 0.10	0.77 ± 0.04
No. of cells	31.3 ± 1.5	32.3 ± 2.2	44.4 ± 5.0	37.6 ± 3.9	51.4 ± 5.8	39.2 ± 2.6
No. of AB stained cell walls	10.3 ± 1.3	13.3 ± 1.7	1.0 ± 1.4	1.0 ± 0.9	2.0 ± 1.7	0.0 ± 0.0
No. of lateral veins	0 ± 0	0 ± 0	0 ± 0	0 ± 0	0.6 ± 0.2	0 ± 0

Data show the average value ± standard errors ($n = 5$). Larger co.: larger cotyledon in a seedling, Smaller co.: smaller cotyledon in a seedling, No. of cells: number of subepidermal cells along the longitudinal axis of a cotyledon, No. of AB stained cell walls: number of Aniline Blue stained cell walls in epi- and subepidermal cells per cotyledon, No. of lateral veins: number of lateral vein bifurcations per cotyledon

cotyledons at 30 DCU (Fig. 2c). Thus, the effects of GA_3 treatment on the cotyledon development were examined in detail up to 10 DCU when the macrocotyledon is clearly distinguishable in the control (Table 1). At this time, the cotyledon area in GA_3 treated seedlings and the smaller cotyledon in control seedlings was statistically indistinguishable ($P = 0.16$).

The number of subepidermal cells along the longitudinal axis was similar in both cotyledons at 1 DCU (control $P = 0.83$; GA_3 treated $P = 0.18$), and became uneven from 5 DCU onwards ($P = 0.01$) (Table 1). There was no statistical difference in the number of cells between the larger and smaller cotyledons in GA_3 treated seedlings ($P = 0.09$), and between GA_3 treated seedlings and those of the microcotyledon in control seedlings 10 DAU ($P = 0.14$).

No lateral veins were observed in the cotyledons of control or GA_3 treated seedlings at 1 and 5 DCU (Table 1).

Fig. 3 **a** Alignment of deduced amino acid sequences of *GA2-oxidase* genes. *SrGA2ox* gene is highly homologous to other class I *GA2-oxidase* genes. The *asterisks* indicate the iron-binding sites (* H-212, D-214 and H-269). Intron positions are marked by *arrowheads*. *SrGA2ox: S. rexii. LsGA2ox1: Latuca sativa*, *SlGA2ox2: S. lycopersicum, AtGA2ox1 A. thaliana*. **b** Neighbor-joining tree based on deduced amino acid sequences of *GA2-oxidase* genes. Bootstrap values (>50 %) of 10,000 replicates are indicated below the branches. I: the class I *GA2-oxidases* gene clade, II: class II *GA2-oxidase* gene clade. *A. thaliana AtGA2ox7* (At1g50960), *AtGA2ox8* (At4g21200), *AtGA2ox2* (At1g30040), *AtGA2ox3* (At2g34555), *AtGA2ox1* (At1g78400), *AtGA2ox6* (At1g02400), *AtGA2ox4* (At1g47990); *Oryza sativa OsGA2ox6* (Os04g0522500), *OsGA2ox5* (Os07g0103500), *OsGA2ox3* (Os01g0757200), *OsGA2ox4* (Os05g0514600), *OsGA2ox2* (Os01g0332300), *OsGA2ox1* (Os05g0158600); *Spinacia oleracea SoGA2ox3* (AAX14674), *SoGA2ox1* (AAN87571), *SoGA2ox2* (AAN87572); *Phaseolus coccineus PcGA2ox* (CAB41036); *Pisum sativum PsGA2bh* (AAF08609), *PsGA2oxlike* (AAD45424); *S. lycopersicum SlGA2ox2* (NM001247409), *SlGA2ox1* (NM001247936), *SlGA2ox3* (NM001247818); *L. sativa LsGA2ox1* (BAB12442); Zea mays *ZmGA2ox* (NM001158585); *S. rexii SrGA2ox*

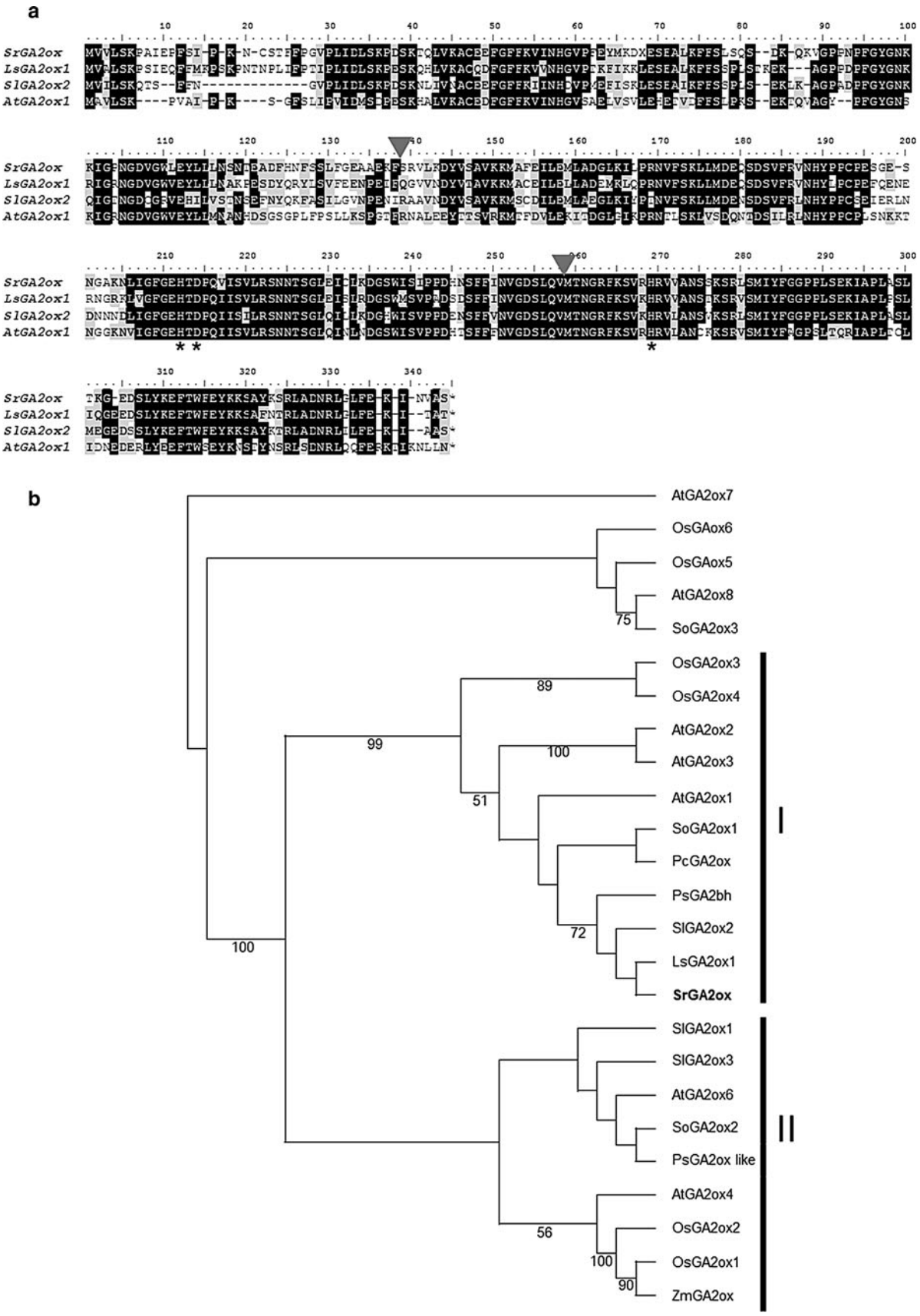
a
SrGA2ox
LsGA2ox1
SlGA2ox2
AtGA2ox1
b
AtGA2ox7
OsGAox6
OsGAox5
AtGA2ox8
SoGA2ox3
OsGA2ox3
OsGA2ox4
AtGA2ox2
AtGA2ox3
AtGA2ox1
SoGA2ox1
PcGA2ox
PsGA2bh
SlGA2ox2
LsGA2ox1
SrGA2ox
SlGA2ox1
SlGA2ox3
AtGA2ox6
SoGA2ox2
PsGA2ox like
AtGA2ox4
OsGA2ox2
OsGA2ox1
ZmGA2ox
I
II
75
89
99
100
51
72
100
56
100
90

At 10 DCU, 2–3 lateral veins had formed in the macrocotyledons of control seedlings, whereas they were rarely observed in cotyledons of GA_3 treated seedlings.

Aniline Blue stained cell walls were observed in the proximal regions of both cotyledons at 1 DCU in control seedlings and GA_3 treated seedlings (Table 1; Online Resource 2). They were continuously observed at the base of the larger cotyledon, whereas they progressively decreased in the smaller cotyledon from 5 DCU to 10 DAU in control seedlings. On the other hand, in GA_3 treated seedlings, they were rarely observed in either cotyledon at 5 DCU or 10 DCU (Table 1; Online Resource 2).

Isolation of *SrGA2ox* and *SrGA20ox*

The full length of the *GA2-oxidase* homolog from *S. rexii*, *SrGA2ox* shared 69.9, 68.6, and 60.9 % identity at the nucleotide level and 71.9, 68.7 and 60.3 % at the deduced amino acid level with *LsGA2ox1* (BAB12442; *Lactuca sativa*), *SlGA2ox2* (NM001247409; *S. lycopersicum*), and *AtGA2ox1* (At1g78400; *A. thaliana*) respectively (Fig. 3a). In addition to the high level of sequence similarity, putative Fe^{2+}-binding sites of 2-oxoglutarate-dependent-dioxigenases (H-212, D-214, H-269), conserved between *GA2-oxidases* (Thomas et al. 1999), were also found in *SrGA2ox* (asterisks in Fig. 3a). Two introns, at the same positions of those in *AtGA2ox1*, were found in *SrGA2ox* (arrowheads in Fig. 3a).

The Neighbor-joining (NJ) tree shows that *SrGA2ox* clearly belongs to the *GA2-oxidase* gene family (Fig. 3b). *GA2-oxidases* are categorized into three classes (I, II, III), according to their hydroxylation site at different carbon positions of gibberellins (Lee and Zeevaart 2005). Class I and II catalyze C_{19}-GAs. In the NJ tree, class I and class II *GA2-oxidases* formed a single clade with 100 % bootstrap support. In this clade, *SrGA2ox* belonged to the class I clade supported with a 99 % bootstrap value (Fig. 3b).

The full length of *GA20-oxidase* isolated from *S. rexii* (*SrGA20ox*) shared 72.3, 71.2, and 60.6 % identity at the nucleotide level with *NtGA20ox* (AB012856; *N. tabacum*), *HaGA20ox1* (AM989990; *Helianthus annuus*), and *AtGA20ox1* (At4g25420; *A. thaliana*), and 76.3, 72.8 and 61.4 % at the amino acid level respectively (Fig. 4a). In the deduced amino acid sequence of *SrGA20ox*, conserved regions between *GA20-oxidase* were found. GA20-oxidase belongs to the 2-oxoglutarate-dependent dioxygenase protein family, and one motif, NYYPPCXXP (positions 242-250, solid underlined in Fig. 4a), is conserved in this gene family, and binds to the common cosubstrate 2-oxoglutarate (Xu et al. 1995). Histidine residues for the Fe^{2+} binding site (H-108, -259, and -315) were also found (asterisks in Fig. 4a; Xu et al. 1995). An LPWKET motif (positions 158-163, double-underlined in Fig. 4a),

Fig. 4 **a** Alignment of deduced amino acid sequence of the conserved region in *GA20-oxidase* genes. The sequence of *SrGA20ox* is highly homologous with *GA20-oxidases*. The *asterisks* indicate putative Fe^{2+} binding sites typical for 2-oxoglutarate-dependent dioxygenases (* H-108, -259, and -315), and *underlines* indicate conserved regions between *GA20-oxidases*. Introns positions were marked by *arrowheads*. *SrGA20ox*: *S. rexii*, *HaGA20ox1*: *H. annuus*, *NtGA20ox*: *N. tabacum*, *AtGA20ox1*: *A. thaliana*. **b** Neighbor-joining tree based on deduced amino acid sequences of *GA20-oxidase* genes. Bootstrap values (>50 %) of 10,000 replicates are indicated below the branches. The *S. rexii GA20-oxidase* (*SrGA20ox*) gene grouped with the dicot *GA20-oxidase* genes. *Chlamydomonas reinhardtii CrFe2/-OG* (Fe/2-OG dependent oxidoreductase XP001695234); *O. sativa OSGA20ox* (AAB48239); *A. thaliana AtGA20ox4* (At1g60980), *AtGA20ox2* (At5g51810), *AtGA20ox1_GA5* (At4g25420); *P. sativum PsGA20ox* (CAA62846); *Fagus sylvatica FsGA20ox1* (CAD21846), *FaGA20ox* (ABB00359); *Populus tremula PtGA20ox1* (CAH59132); *Malus x domestica MdGA20ox* (BAB20975); *H. annuus HaGA20ox2* (CAQ43617), *HaGA20ox1* (AM989990); *S. lycopersicum SlGA20ox3* (AAD15756), *SlGA20ox1* (AAD15755); *N. tabacum NtGA20ox_Ntc16* (AB012856), *NtGA20ox_Ntc12* (BAA31689); *S. rexii SrGA20ox*

conserved between *GA20-oxidases*, thought to be involved in binding to the substrates of gibberellins (Xu et al. 1995), was also identified in *SrGA20ox*. Two introns were found at the same positions as those in *HaGA20ox1* (arrowheads in Fig. 4a; see Carzoli et al. 2009). The Neighbor-joining tree of *GA20-oxidases* indicated that *SrGA20ox* belongs to *GA20-oxidase* genes (Fig. 4b). The dicot clade of *GA20-oxidase* genes, including *SrGA20ox*, was supported by a 90 % bootstrap value. *SrGA20ox* is closely related here to the *GA20-oxidases* of Lamiales species, such as tobacco (*Ntc12*, *Ntc16*) or tomato (*SlGA20ox1*, *SlGA20ox3*) though with a low bootstrap value (54 %).

In situ expression patterns of *SrGA2ox* and *SrGA20ox* during embryogenesis

During embryogenesis, at the transition between globular to heart stage, *SrGA2ox* expression was observed in the cotyledon primordia and in the distal end of the embryo (Fig. 5a). Early heart stage embryos showed *SrGA2ox* expression in the cotyledon primordia, in the procambium, and at the distal end (Fig. 5b). At the heart stage, *SrGA2ox* was predominantly expressed at the distal end of both cotyledons and at the lower distal end of the embryo, and in procambium (Figs. 5c, d, 10). This pattern continued during the heart stage (Figs. 5e, 10). At the early linear cotyledon stage, serial sections showed *SrGA2ox* expression on the adaxial side of both cotyledons, with the signal decreasing at the junction between hypocotyl and cotyledons (Figs. 5f–h, 10). At the late linear cotyledon stage, *SrGA2ox* was restricted to the adaxial side and here more in the proximal region of both cotyledons (Figs. 5i, j, 10). In transverse sections, *SrGA2ox* expression appeared to be focused in two regions near the base of the cotyledons

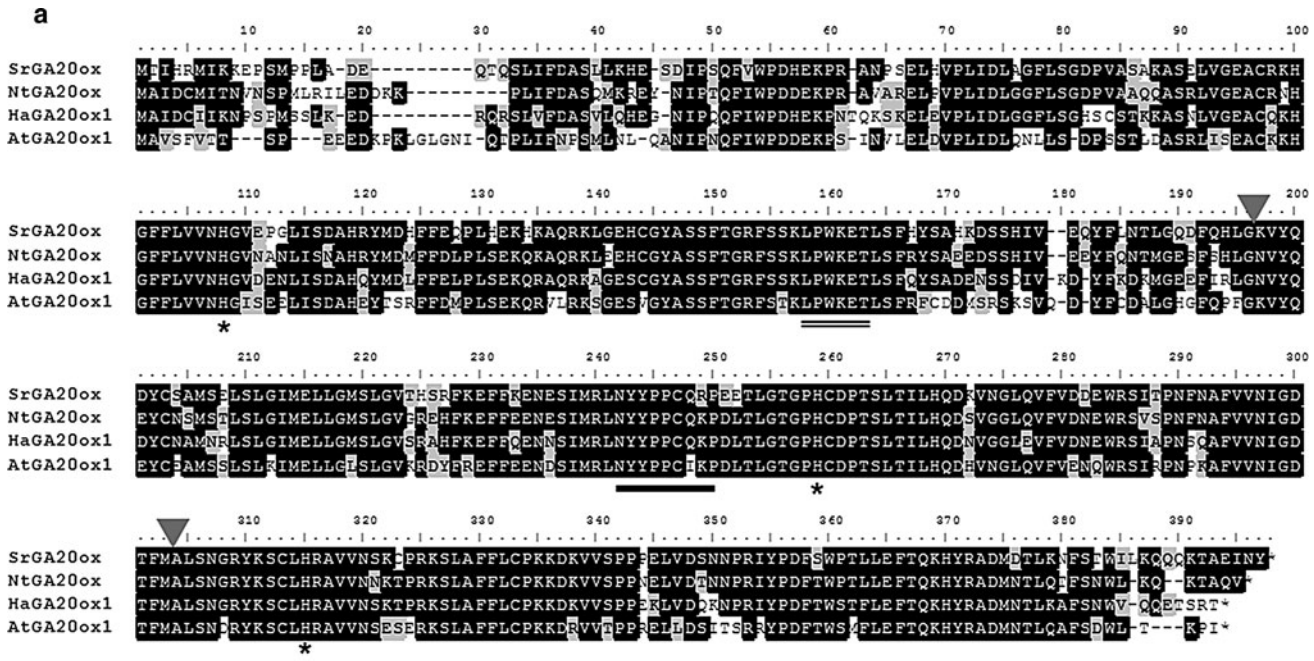
a
SrGA20ox
NtGA20ox
HaGA20ox1
AtGA20ox1

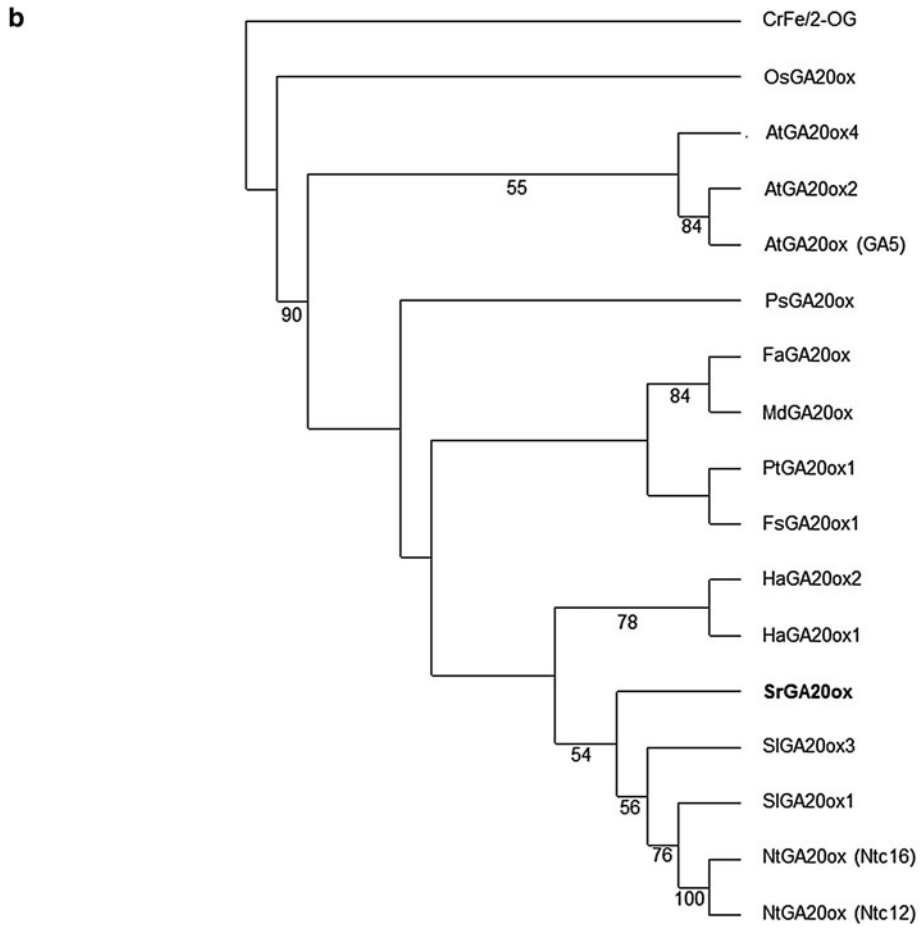
b
CrFe/2-OG
OsGA20ox
AtGA20ox4
AtGA20ox2
AtGA20ox (GA5)
PsGA20ox
FaGA20ox
MdGA20ox
PtGA20ox1
FsGA20ox1
HaGA20ox2
HaGA20ox1
SrGA20ox
SlGA20ox3
SlGA20ox1
NtGA20ox (Ntc16)
NtGA20ox (Ntc12)
55
84
90
84
78
54
56
76
100

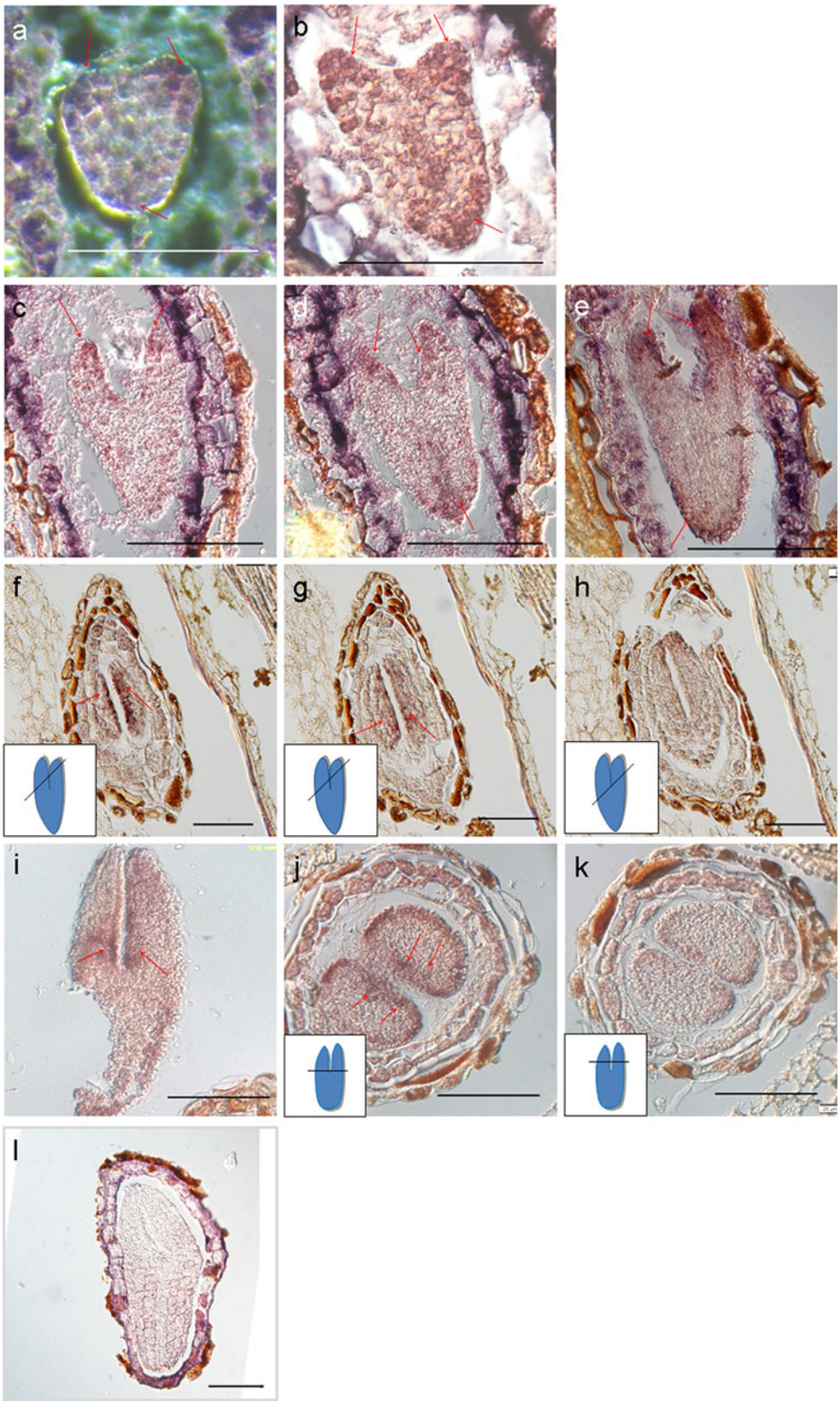
a
b
c
d
e
f
g
h
i
j
k
l

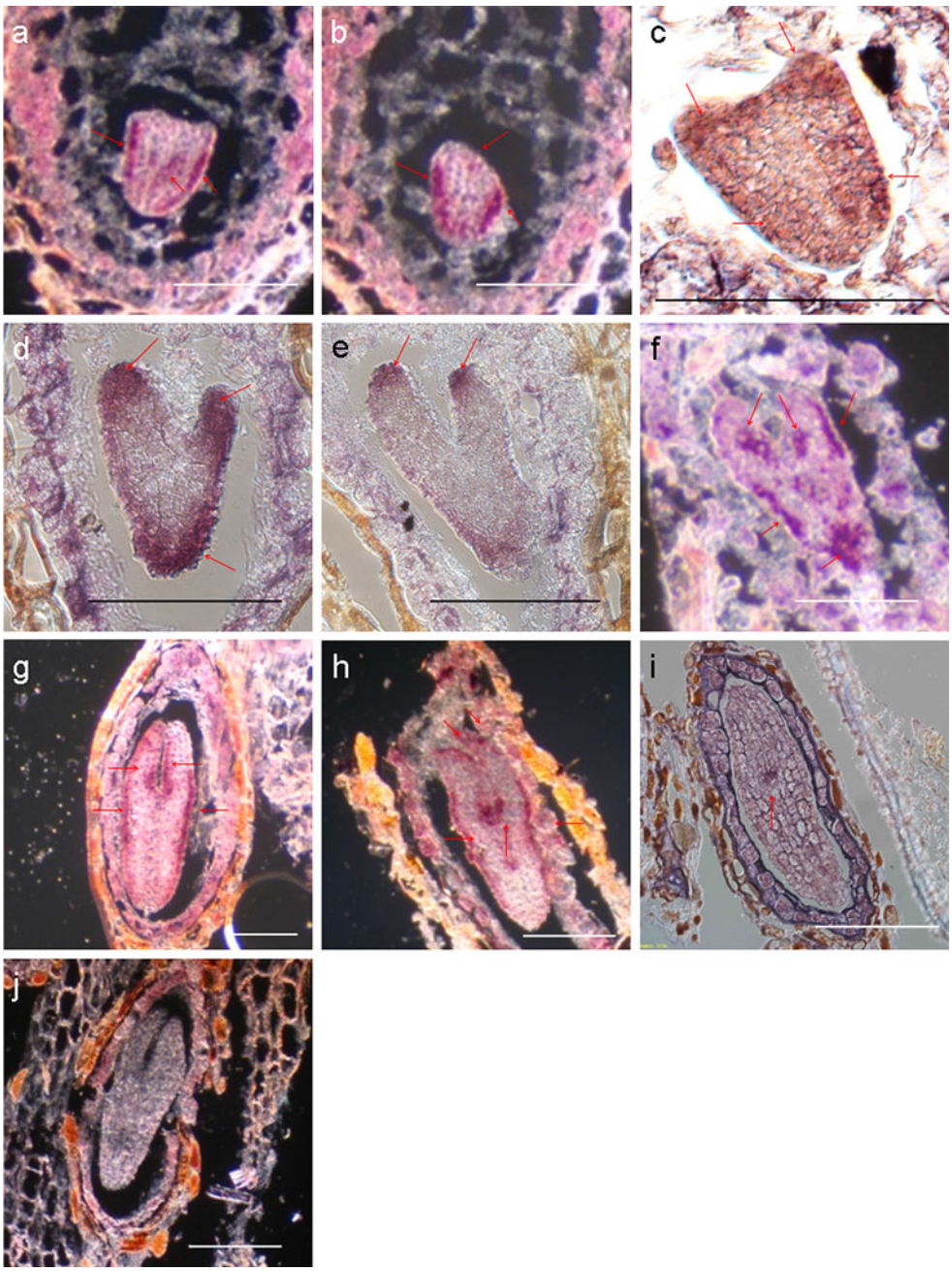

Fig. 6 In situ hybridization of *SrGA20ox* in developing embryos of *S. rexii*. **a–c** LSs of transition between globular to heart stage embryos. **a**, **b** Serial LSs of same embryo. **c** LS of another embryo. **d**, **e** LSs of heart stage embryos. **d** LS of slightly outside of mid-plane. **e** LS of mid-plane. **f** LS of late heart stage embryo. **g, h** LSs of early linear cotyledon stage embryos. **i** LS of linear cotyledon stage embryo. **j** LS of mature embryo. *Bars* 100 μm. *Arrows* indicate the in situ hybridization signals of *SrGA20ox*

◀ **Fig. 5** In situ hybridization of *SrGA2ox* in developing embryos of *S. rexii*. **a** Longitudinal section (LS) of transition between globular to heart stage embryo. **b** LS of early heart stage embryo. **c**, **d** Serial LSs of heart stage embryo. **c** Section slightly outside from the mid-plane. **d** Mid-plane section. **e** LS of late heart stage embryo. **f–h** Serial sections of early linear cotyledon stage. *Inset* illustrations indicate the plane of sectioning. **i** LS of linear cotyledon stage. **j**, **k** Transverse sections (TSs) of linear cotyledon stage embryo. *Inset* illustrations indicate the plane of sectioning. **l** LS of mature embryo. *Bars* 100 μm. *Arrows* indicate the in situ hybridization signals of *SrGA2ox*

(Figs. 5j, 10), but weak in the section of the cotyledon tip (Fig. 5k). In mature embryos, *SrGA2ox* expression was not observed (Fig. 5l). The sections hybridized with sense transcribed RNA probes for negative control did not show the purple or blue signals (Online resource 3).

SrGA20ox was observed in the outer layers of the embryo at the transition between globular and heart stage (Figs. 6a–c, 10). Stronger signals were observed in the

lateral epidermal areas of the embryo (Fig. 6a, b), and expanded to the lateral area (Figs. 6c, 10). At the heart stage, *SrGA20ox* expression was observed in the tip of both cotyledons and in the outer layers of the embryo in off mid-plane sections (Fig. 6d), and was restricted to the tip of both cotyledons and the distal part of the embryo in mid-plane sections (Figs. 6e, 10). At the late heart stage, *SrGA20ox* expression was restricted to the adaxial layers of the proximal region of both cotyledons, to the outer abaxial layers of the cotyledons and the lower distal end of the embryo (Figs. 6f, 10). At the early linear cotyledon stage, *SrGA20ox* expression was more focused in the proximal-adaxial region between the two cotyledons and the outer layers of the embryo, an area corresponding to the abaxial layers of both cotyledons and the hypocotyl region (Figs. 6g, h, 10). Intriguingly, at the linear embryo stage, *SrGA20ox* expression was restricted entirely to a central region between the two cotyledons (Figs. 6i, 10). It was not observed in the mature embryo (Fig. 6j), or in sections hybridized with sense transcribed RNA probes of negative controls (Online resource 4).

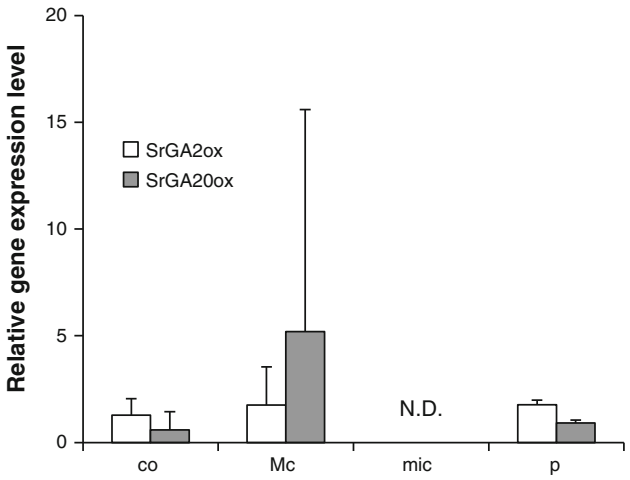

Fig. 7 Real-time PCR expression patterns of *SrGA2ox* (*open bars*) and *SrGA20ox* (*shaded bars*) in developing cotyledons and newly formed phyllomorphs of *S. rexii*. Relative expression levels against the whole seedling are calculated using *18SrRNA* as internal control ($n = 3$). co: cotyledons in isocotylous seedling, Mc: macrocotyledon, mic: microcotyledon, p: newly formed phyllomorph, N.D.: not detected

Spatial–temporal expression patterns of *SrGA2ox* and *SrGA20ox* during seedling development

Real-time PCR results showed that both genes were expressed in the cotyledons of isocotylous seedlings, and in the macrocotyledon of anisocotylous seedling at 40 DCU, but not in the microcotyledon at this stage of development (Fig. 7). Expression of *SrGA2ox* and *SrGA20ox* was also detected in newly formed phyllomorphs.

In situ hybridization showed that just after germination *SrGA2ox* expression was observed on the adaxial side of both cotyledons (Figs. 8a, b, 10). At 7 DCU, when anisocotyly became apparent, *SrGA2ox* was observed in the basal meristem region of the developing macrocotyledon (Figs. 8c, d, 10). In strongly anisocotylous seedling, 35 DAU, *SrGA2ox* was present in the basal meristem and the groove meristem (Figs. 8e–g, 10). In GA_3 treated isocotylous seedlings, *SrGA2ox* expression was restricted to the new phyllomorph primordia developing between the cotyledons but not in cotyledons (Fig. 8h).

SrGA20ox expression was observed broadly in both cotyledons of seedlings at the isocotylous stage (Figs. 9a, b, 10). In seedlings at 7 DCU, when the basal meristem started to be distinguishable, *SrGA20ox* expression was excluded from the area of the basal meristem (Figs. 9c, d, 10). In anisocotylous seedlings, an *SrGA20ox* signal was only observed in the distal region (Figs. 9e, f, 10), and not in the proximal region of the macrocotyledon (asterisk in Fig. 8f). Negative controls hybridized with sense transcribed *SrGA2ox* or *SrGA20ox* showed a brown background colour, but did not show a blue or purple in situ coloured signal (Online Resource 3, 4).

Effect of hormone treatments on *SrGA2ox* and *SrGA20ox* expression levels

GA_3 treatment caused a strong up-regulation of *SrGA2ox* [$P(H1) < 0.0001$]. A weaker but similar effect was observed after BAP treatment [$0.01 < P(H1) < 0.05$] (Fig. 11). On the contrary, the expression levels of *SrGA20ox* were not affected by either hormone treatment (Fig. 11).

Discussion

Lack of SAM and the development of novel meristems in *S. rexii*

Previous studies have shown that an embryonic or post-embryonic SAM is not observed in *S. rexii* (e.g. Jong 1970), and no plumula is present between the cotyledons after germination (Fig. 1). However, the seedlings develop a basal meristem in the lamina of cotyledons, which serves to rapidly expand the photosynthetic organs (Burtt 1970). The interesting aspect of our study is that both cotyledons initially possess a basal meristem, but continued division occurs only in one cotyledon to form the macrocotyledon. In this study, we tried to link the unique meristem occurrence of *S. rexii* with GA synthesis/degradation genes. These are known to be associated with developmental

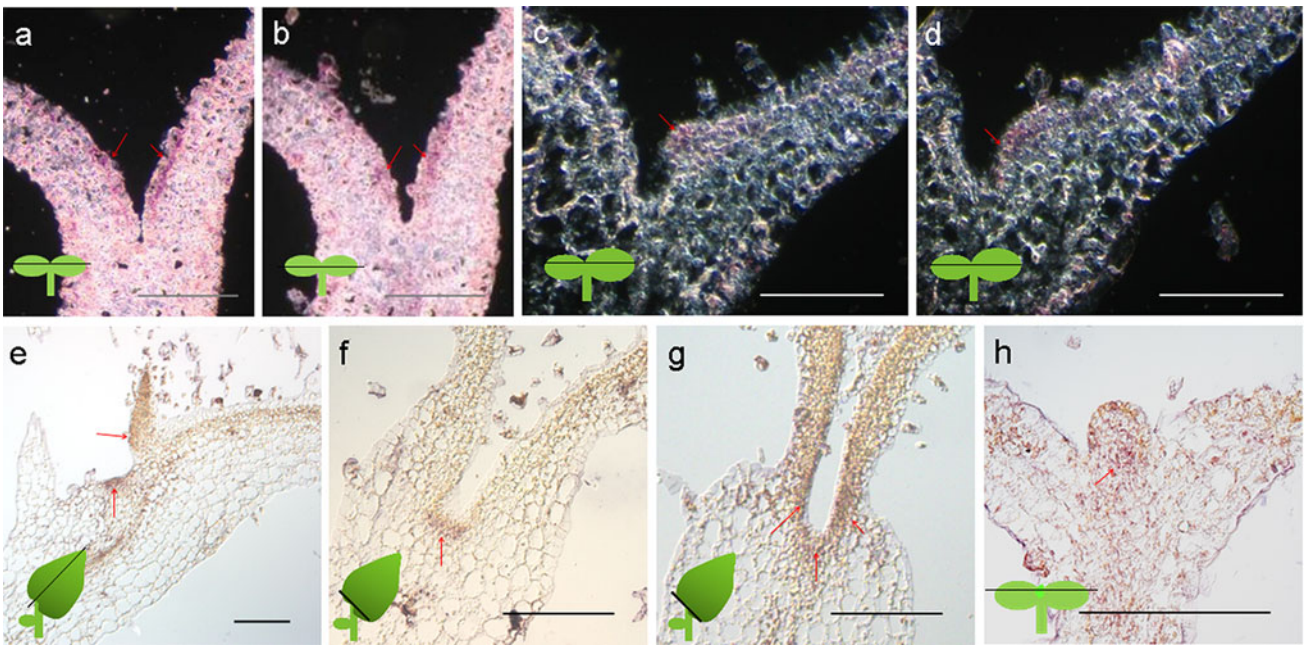

Fig. 8 *In situ* hybridization of *SrGA2ox* in developing seedlings of *S. rexii*. **a**, **b** Serial LSs of a seedling just after germination (3 DCU). **c**, **d** Serial LSs of a seedling at the beginning of anisocotyly (7DCU). **e**–**g** Anisocotylous stage (35 DCU). **e** LS of an anisocotylous seedling. **f**, **g** Serial TSs of the proximal region of the macrocotyledon. **h** LS of GA_3 treated seedling. *Bars* 100 µm. *Arrows* indicate in situ hybridization signals of *SrGA2ox*

genes in model plants (Hay et al. 2002; Jasinski et al. 2005).

Exogenous GA treatment modulate meristems formation in *S. rexii*

Exogenous GA_3 treatment altered the meristem formation and maintenance in the cotyledons of *S. rexii.* In GA_3 treated seedlings, both cotyledons remained smaller (Fig. 2), similar to the microcotyledons of normally developing seedlings. This was due to a reduced cell division rate, causing a suppression of the basal meristem (Table 1; Fig. 2; Online Resource 2). This GA effect is consistent with previous observations on the plurifoliate *Streptocarpus prolixus* (Rosenblum and Basile 1984), and the unifoliate *Streptocarpus wendlandii* (Nishii et al. 2012). Thus, all species of the genus appear to share a common mechanism to switch from anisocotyly to isocotyly in the presence of excess amounts of GA, by negatively regulating the basal meristem activity.

SrGA2ox and *SrGA20ox* as the homologs of *GA2-oxidase* and *GA20-oxidase* genes

The gene homology analyses on *SrGA2ox* and *SrGA20ox* (i.e. sequence similarity, conservation of recognition domains, and phylogenetic relatedness), all strongly indicated that the *SrGA2ox* and *SrGA20ox* sequences we isolated here, are homologs of *GA2-oxidase* and *GA20-oxidase*, respectively. Specifically, the isolated *SrGA2ox* grouped with *GA2-oxidases* catabolizing C_{19}-GAs (Lee and Zeevaart 2005), which has been shown to be a major mechanism in GA inactivation in *Arabidopsis* (Rieu et al. 2008). On the contrary, *SrGA20ox* fell among other *GA20-oxidases* that are responsible for the production of active GA, C_{19}-GAs (Yamaguchi 2008).

SrGA2ox and *SrGA20ox* expression patterns during embryogenesis

During the embryogenesis, *SrGA2ox* and *SrGA20ox* expression patterns dynamically changed over the developmental stages in *S. rexii*. Both genes were expressed in the cotyledons and at the distal end of the embryo in early embryogenesis stages (Figs. 5a, b, 6a–c, 10a, f). However, a more spatial separation occurred over time (Figs. 5, 6, 10). At the early heart stage, the expression of *SrGA2ox* was observed more in the mid plane, while *SrGA20ox* more in the section slightly outside the mid-plane. Thus, though the expression of *SrGAox* and *SrGA20ox* seemed to overlap at that stage, the expression patterns of *SrGA2ox* and *SrGA20ox* appeared rather complementary in three dimensions (Figs. 5c, d, 6d, e). At the late embryogenesis stages, the expression of the two genes was even more localized and each gene had a more narrower expression domain in the embryo (Fig. 10d, e, i, j), which is likely

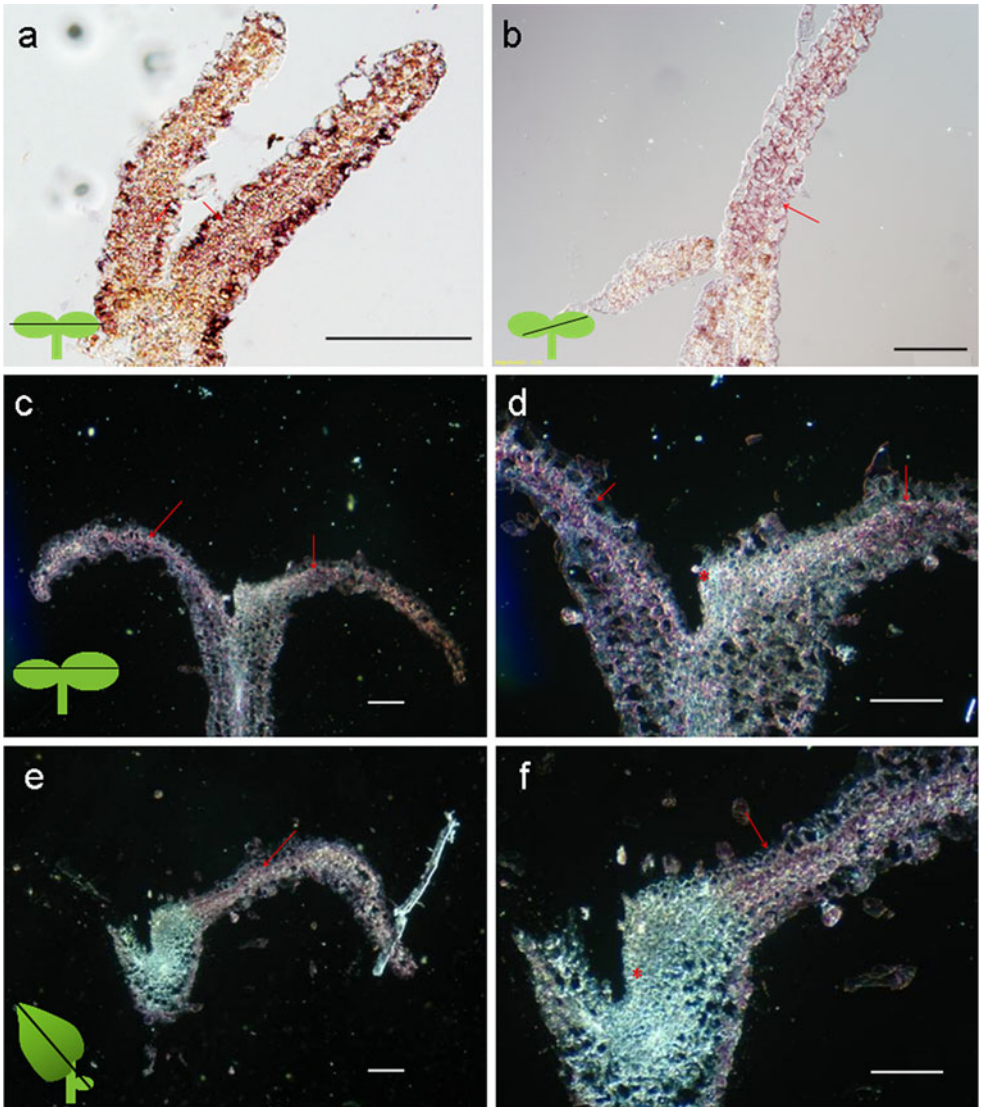

Fig. 9 In situ hybridization of *SrGA20ox* in developing seedlings of *S. rexii*. **a** LS of isocotylous stage seedling (3 DCU). **b** Oblique LS of isocotylous seedling. **c** LS of seedling at the beginning of the anisocotylous stage (7 DCU). **d** Magnified image of adjacent section to **c**. *GA20-oxidase* expression is not detected in the proximal region of the macrocotyledon (*asterisk*). **e**, **f** LS through anisocotylous stage seedling (35 DCU). **f** Magnified view of **e**. *SrGA20ox* expression is not detected where the basal meristem or the groove meristem is located in the macrocotyledon (*asterisk*). *Bars* 100 µm. *Arrows* indicate in situ hybridization signals of *SrGA20ox*

related to their differential functions. Thus, over time the expression patterns became mutually exclusive towards to the end of embryogenesis. It is particularly interesting that the *SrGA20ox* expression was basically restricted to a small area between the cotyledons towards the end of embryo development (Figs. 6i, 10j), where ordinary plants form an embryonic SAM, while *SrGA2ox* expression occurred in the putative meristematic area of *S. rexii* in the adaxial-proximal side of cotyledons (Fig. 5i, j, 10e). This suggests that GA concentrations regulated by *SrGA20ox* and *SrGA2ox* might have some role for preventing the formation of a SAM and laying the foundations for a basal meristem in the embryo of *S. rexii*.

The expression patterns of *SrGA2ox* and *SrGA20ox* in *S. rexii* are unique compared to those found in other species with a SAM. In *A. thaliana*, *AtGA2ox6* expression was detected across heart stage embryos and appeared to be weaker in the cotyledons (Wang et al. 2004), much in contrast to *S. rexii* here (Fig. 10b, c). In runner beans, the expression of *PcGA2ox1* was observed in the suspensor but not in the cotyledon of early cotyledon stage embryos (Solfanelli et al. 2005). In pumpkins, *GA20-oxidase*

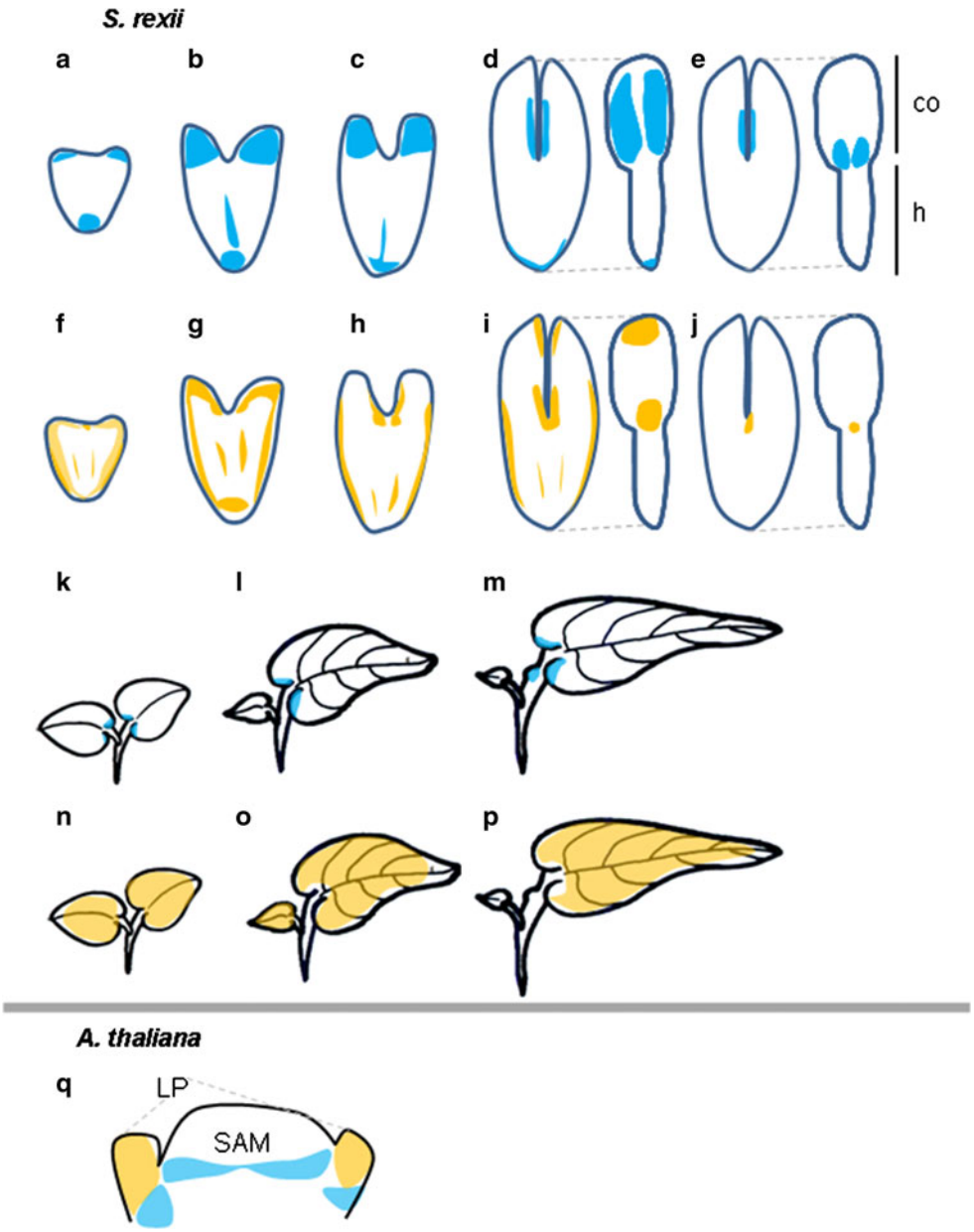

Fig. 10 Schematic illustration of the observed expression patterns of *GA oxidases*. **a–p** Expression patterns of *SrGA2ox* (*blue*) and *SrGA20ox* (*orange*) in *S. rexii*. **a–e**, **k–m** *SrGA2ox* **f–j**, **n–p** *SrGA20ox* **a**, **f** Transition from globular to heart embryo stage. **b**, **g** Early heart embryo stage. **c**, **h** Late heart embryo stage. **d**, **i** Early linear cotyledon stage. **e**, **j** Late linear cotyledon stage. **d**, **e**, **i**, **j** Front (*left side*) and side views (*right side*), rotated 90° around the longitudinal axis, are given. co: cotyledon part of embryo, h: hypocotyl part of embryo. **k**, **n** Seedlings just after germination. **l**, **o** Seedlings at the beginning of anisocotylous stage. **m**, **p** Anisocotylous seedlings. **q** Expression of *GA2-oxidase* (blue) and *GA20-oxidase* in the SAM of *A. thaliana*, modified from Hay et al. (2002) and Jasinski et al. (2005). SAM: shoot apical meristem, LP: leaf primordia

expression was found not focused between the cotyledons, where the SAM is established (Frisse et al. 2003). All these reports indicate that *GA20-oxidase* expression is not present or never focused in the location where the SAM occurs, and that *GA2-oxidase* expression is weak or absent in cotyledon primordia. This is in contrast to our findings and suggesting a possible direct role of GA in the peculiar development of *S. rexii*.

SrGA2ox and *SrGA20ox* expression patterns during germination

The expression of *SrGA2ox* and *SrGA20ox* during germination was clearly mutually exclusive. Just after germination, *SrGA2ox* expression was observed only in the adaxial-proximal side of both cotyledons, while *SrGA20ox* expression was more widespread in the lamina of cotyledons. At the onset of anisocotyly, *SrGA2ox* expression was solely observed in the basal meristem of the macrocotyledon. In the established macrocotyledon or phyllomorphs, *SrGA2ox* was besides localized in the basal meristem, also found in the groove meristem. On the other hand, *SrGA20ox* expression was never found in meristematic areas, but in the developing lamina. This suggests that *SrGA2ox* and *SrGA20ox* have contrasting roles for the meristem formation and maintenance in the seedlings after germination, as well as in the embryo of *S. rexii*.

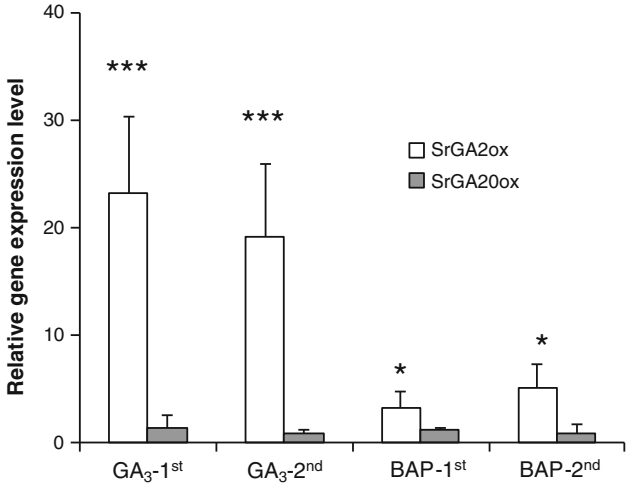

Fig. 11 Real-time PCR expression patterns of *SrGA2ox* (*open bars*) and *SrGA20ox* (*shaded bars*) in the cotyledonary phyllomorphs (the macrocotyledon) of *S. rexii* seedlings treated with gibberellin (GA_3) or cytokinin (BAP). The relative gene expression levels were calculated against untreated cotyledonary phyllomorphs ($n = 3$). Two biological repeats are shown (1st, 2nd). * [$0.01 < P(H1) < 0.05$] or *** [$P(H1) < 0.0001$] indicate level of significances to control samples. Treatments without *asterisks* did not show statistically significant differences to control samples

Hormonal control of *SrGA2ox* and *SrGA20ox*

SrGA2ox was up-regulated by exogenous application of GA (GA_3) or CK (BAP) (Fig. 11). GA_3, in particular, strongly increased *SrGA2ox* expression levels. In *A. thaliana*, GA treatments also increased C_{19}-GA2-oxidases, such as *AtGA2ox1*, *AtGA2ox2*, and *AtGA2ox4* (Thomas et al. 1999; Rieu et al. 2008). Thus, *SrGA2ox* appears to possess a feed-back loop, sensing and removing excess amounts of GA. BAP treatments also induced an *SrGA2ox* up-regulation in *S. rexii* seedlings, as in *A. thaliana*, where a BAP treatment increased *AtGA2ox2* expression around the SAM (Jasinski et al. 2005).

Although some *GA20-oxidases* are negatively regulated by hormone treatment in several plants, we could not detect an alteration of the *SrGA20ox* expression level after GA_3 or BAP treatment. However, it is not yet known whether *S. rexii* retains redundant *GA20-oxidases* that would respond to hormone treatments. In several plants, redundant *GA20-oxidases* were found responding differently to hormone treatments. In tobacco, for example, *GA20-oxidase Ntc12* expression was negatively affected by GA_3 or the GA inhibitor uniconazol, but not by another *GA20-oxidase Ntc16* (Tanaka-Ueguchi et al. 1998). In *H. annuus*, the expression level of *HaGA20ox2* was found to be negatively affected by the GA inhibitor paclobutrazol, but not that of *HaGA20ox1* (Carzoli et al. 2009). Since the expression of our isolated *SrGA20ox* was not affected by hormonal treatment, it might be regulated by another pathway (e.g. KNOX1 protein; see below).

GA metabolic genes along with *KNOX1* genes express unorthodoxly in the phyllomorphic *S. rexii*

In the model plant *A. thaliana*, the *KNOX1* gene *SHOOT-MERISTEMLESS* (*STM*) is expressed in the cotyledon fork, starting from heart stage embryo, and is maintained throughout meristem persistence (Long et al. 1996; Hake et al. 2004). Studies on the *STM* ortholog of *S. rexii*, *SrSTM1* showed that it is expressed in the cotyledons but not in the cotyledon fork. In developing seedlings, *SrSTM1* is first expressed in both cotyledons and later only in the basal meristem and the groove meristem of the macrocotyledon (Mantegazza et al. 2007). Another *KNOX1* gene studied in *S. rexii*, *SrBP* followed this expression patterns (Nishii et al. 2010). In this study, the expressions of *SrGA2ox* were found to be partly overlapping with those of the two *KNOX1* genes. On the other hand, *SrGA20ox* as a *SrGA2ox* antagonist, is consequently excluded from the meristems.

The link between *KNOX1* and GA metabolism genes has been reported in model plants. In tobacco, overexpression of *NTH15* reduced the expression level of the *GA20-oxidase*, *Ntc12* (Tanaka-Ueguchi et al. 1998), through NTH15 protein binding to the intron of *Ntc12* (Sakamoto et al. 2001a). In rice, direct regulation of *GA2ox1* by the *KNOX1* gene, *KN1*, has been reported; *KNOX1* binds to TGAC motifs in the 1st intron of *GA2ox1* (Bolduc and Hake 2009). Interestingly, we found three TGAC motifs in the 2nd intron of *SrGA2ox* (Online Resource 5) and in the 2nd intron of *SrGA20ox* (Online Resource 6). Further studies may reveal their role in the regulatory mechanism of *KNOX1* genes on the GA metabolism pathway in *S. rexii*.

Our data suggest that, in *S. rexii*, the *KNOX1* and GA regulatory pathways coordinated the sculpturing of the plant's unique morphology. *KNOX1* expression followed the meristem positions during embryogenesis and seedling development (Mantegazza et al. 2007; Nishii et al. 2010). This correlation was maintained in the meristems in the macrocotyledon and phyllomorphs. The expression of the GA degradation gene, *SrGA2ox*, overlapped with the *KNOX1* expression patterns, but more narrower, reminiscent of the situation in *A. thaliana*. In *A. thaliana*, *STM* is expressed in the entire SAM, and *GA2-oxidase* is located at the base of the SAM to prevent GA translocation into the SAM (Jasinski et al. 2005). In *S. rexii*, the GA synthesis gene, *SrGA20ox*, on the other hand, was excluded from the meristem region and expressed in the lamina. This suggests high GA concentrations in the lamina preventing meristematic activity, that coincided with a transfer to cell determinacy and lamina expansion, as in *A. thaliana* (Jasinski et al. 2005).

Conclusions

In this study, we analyzed the expression of GA synthesis and degradation genes during the meristem formation in *S. rexii*. Our results suggest that they are associated with the suppression of an embryonic SAM and the formation and maintenance of unique meristems in *S. rexii*. The results further suggest that low levels of GA are required for their establishment and maintenance. Thus, the meristems in *S. rexii* may share some regulatory pathways characterized for the SAM in model plants. In *S. rexii*, however, evolutionary modifications involving a lateral transfer of meristem function, from shoot to leaves, is implicated in attaining the unusual morphology of the plants.

Since *KNOX1* genes have also been found expressed in leaf meristems in *S. rexii*, perhaps the regulatory pathways of *KNOX1* and *GA-oxidase* genes interact. In this scenario of crosstalk between hormone signaling and developmental genes in the formation and maintenance of meristems, some aspects may have been conserved between the model plant *Arabidopsis* and the non-model plant *S. rexii*, and their unusual shape may have come about by step-wise spatial–temporal changes over evolutionary time.

Acknowledgments This work was supported, in part, by a Taiwan-Italy Scientific Research Cooperation grant from the National Science Council (NSC) in Taiwan and National Research Council (CNR) in Italy (Grant Number 99-2923-B-002-007-MY2) and the Excellent Research Program from the National Taiwan University (10R30701, NTU) to CW. KN is supported by the NSC funding NSC 101-2811-B-002-150 and Sibbald Trust at Royal Botanic Garden Edinburgh (UK). We thank Dr. Min-Liang Kuo (NTU), Dr. Shin-Tong Jeng (NTU), Dr Tsan-Piao Lin (NTU) and Dr. Shih-Ying Hwang (National Taiwan Normal University, Taiwan) for their research funding support and helpful comments on this study. We thank Dr. K.-J. Tang and Ms. Y.-Y. Gao (TechComm, NTU) for technical support and enabling access to real-time PCR facilities. We thank the Science Division of RBGE for supporting this work. RBGE is supported by the Rural and Environment Science and Analytical Services division (RESAS) in the Scottish Government.

References

Bolduc N, Hake S (2009) The maize transcription factor *KNOTTED1* directly regulates the gibberellin catabolism gene *ga2ox1*. Plant Cell 21:1647–1658

Burtt BL (1970) Studies in Genseriaceae of the old world XXXI: some aspect of functional evolution. Notes R Bot Gard Edinb 30:1–10

Carzoli FG, Michelotti V, Fambrini M, Salvini M, Pugliesi C (2009) Molecular cloning and organ-specific expression of two Gibberellin 20-oxidase genes of *Helianthus annuus*. Plant Mol Biol Rep 27:144–152

Cutler DF, Botha T, Stevenson DW (2007) Plant anatomy: an applied approach. Blackwell Publishing, Oxford

Frisse A, Pimenta MJ, Lange T (2003) Expression studies of gibberellin oxidases in developing pumpkin seeds. Plant Physiol 131:1220–1227

Hake S, Smith HMS, Holtan H, Magnani E, Mele G, Ramirez J (2004) The role of *KNOX* genes in plant development. Annu Rev Cell Dev Biol 20:125–151

Harrison J, Möller M, Langdale J, Cronk Q, Hudson A (2005) The role of *KNOX* genes in the evolution of morphological novelty in *Streptocarpus*. Plant Cell 17:430–443

Hay A, Kaur H, Phillips A, Hedden P, Hake S, Tsiantis M (2002) The gibberellin pathway mediates KNOTTED1-type homeobox function in plants with different body plans. Curr Biol 12:1557–1565

Hayashi T, Polonenko DR, Camirand A, Maclachlan G (1986) Pea xyloglucan and cellulose IV. Assembly of ß-glucans by pea protoplasts. Plant Physiol 82:301–306

Imaichi R, Nagumo S, Kato M (2000) Ontogenetic anatomy of *Streptocarpus grandis* (Gesneriaceae) with implications for evolution of monophylly. Ann Bot 86:37–46

Jasinski S, Piazza P, Craft J, Hay A, Woolley L, Rieu I, Phillips A, Hedden P, Tsiantis M (2005) *KNOX* action in *Arabidopsis* is mediated by coordinate regulation of cytokinin and gibberellin activities. Curr Biol 15:1560–1565

Jong K (1970) Developmental aspects of vegetative morphology of *Streptocarpus.* PhD dissertation, University of Edinburgh

Jong K, Burtt BL (1975) The evolution of morphological novelty exemplified in the growth patterns of some Gesneriaceae. New Phytol 75:297–311

Jürgens G (2001) Apical-basal pattern formation in *Arabidopsis* embryogenesis. EMBO J 20:3609–3616

Kuwabara A, Nagata T (2006) Cellular basis of developmental plasticity observed in heterophyllous leaf formation of *Ludwigia arcuata* (Onagraceae). Planta 224:761–770

Lavoie H, Hogues H, Mallick J, Sellam A, Nantel A, Whiteway M (2010) Evolutionary tinkering with conserved components of a transcriptional regulatory network. PLoS Biol 8:e1000329

Lee DJ, Zeevaart JAD (2005) Molecular cloning of *GA 2-Oxidase3* from spinach and its ectopic expression in *Nicotiana sylvestris*. Plant Physiol 138:243–254

Long JA, Moan EI, Medford JI, Barton MK (1996) A member of the KNOTTED class of homeodomain proteins encoded by the *STM* gene of *Arabidopsis*. Nature 379:66–69

Mantegazza R, Möller M, Harrison CJ, Fior S, De Luca C, Spada A (2007) Anisocotyly and meristem initiation in an unorthodox plant, *Streptocarpus rexii* (Gesneriaceae). Planta 225:653–663

Mantegazza R, Tononi P, Möller M, Spada A (2009) *WUS* and *STM* homologs are linked to the expression of lateral dominance in the acaulescent *Streptocarpus rexii* (Gesneriaceae). Planta 230:529–542

Nishii K, Nagata T (2007) Developmental analyses of the phyllomorph formation in the rosulate species *Streptocarpus rexii* (Gesneriaceae). Plant Syst Evol 265:135–145

Nishii K, Kuwabara A, Nagata T (2004) Characterization of anisocotylous leaf formation in *Streptocarpus wendlandii* (Gesneriaceae): significance of plant growth regulators. Ann Bot 94:457–467

Nishii K, Möller M, Kidner CA, Spada A, Mantegazza R, Wang C-N, Nagata T (2010) A complex case of simple leaves: indeterminate leaves co-express *ARP* and *KNOX1* genes. Dev Gen Evol 220:25–40

Nishii K, Wang C-N, Spada A, Nagata T, Möller M (2012) Gibberellin as a suppressor of lateral dominance and inducer of apical growth in the unifoliate *Streptocarpus wendlandii* (Gesneriaceae). N Z J Bot 50:267–287

Ochman H, Gerber AS, Hart DL (1988) Genetic applications of an inverse polymerase chain reaction. Genetics 120:621–623

Olszewski N, Sun T-P, Gubler F (2002) Gibberellin signaling: biosynthesis, catabolism, and response pathways. Plant Cell 14:S61–S80

Park S, Harada JJ (2008) *Arabidopsis* embryogenesis. Methods Mol Biol 427:3–16

Pfaffl MW, Horgan GW, Dempfle L (2002) Relative expression software tool (REST) for group-wise comparison and statistical analysis of relative expression results in real-time PCR. Nucleic Acids Res 30:E36

Rieu I, Eriksson S, Powers SJ, Gong F, Griffiths J, Woolley L, Benlloch R, Nilsson O, Thomas SG, Hedden P, Phillipsa AL (2008) Genetic analysis reveals that C_{19}-GA 2-oxidation is a major gibberellin inactivation pathway in *Arabidopsis*. Plant Cell 20:2420–2436

Rosenblum IM, Basile DV (1984) Hormonal-regulation of morphogenesis in *Streptocarpus* and its relevance to evolutionary history of the Gesneriaceae. Am J Bot 71:52–64

Sakamoto T, Kamiya N, Ueguchi-Tanaka M, Iwahori S, Matsuoka M (2001a) KNOX homeodomain protein directly suppresses the expression of a gibberellin biosynthetic gene in the tobacco shoot apical meristem. Genes Dev 15:581–590

Sakamoto T, Kobayashi M, Itoh H, Tagiri A, Kayano T, Tanaka H, Iwahori S, Matsuoka M (2001b) Expression of a gibberellin 2-oxidase gene around the shoot apex is related to phase transition in rice. Plant Physiol 125:1508–1516

Schneider CA, Rasband WS, Eliceiri KW (2012) NIH Image to ImageJ: 25 years of image analysis. Nat Methods 9:671–675

Solfanelli C, Ceron F, Paolicchi F, Giorgetti L, Geri C, Ceccarelli N, Kamiya Y, Picciarelli P (2005) Expression of two genes encoding gibberellin 2- and 3-oxidases in developing seeds of *Phaseolus coccineus*. Plant Cell Physiol 46:1116–1124

Staheli JP, Boyce R, Kovarik D, Rose TM (2011) CODEHOP PCR and CODEHOP PCR primer design. In: Park DJ (ed) PCR protocols (Methods in molecular biology), vol 687. Humana Press, New York, pp 57–73

Steeves TA, Sussex IM (1989) Patterns in plant development. Cambridge University Press, New York

Swofford DL (2002) PAUP*: Phylogenetic analysis using parsimony (*and other methods), version 4.0b10. Sinauer Associates, Sunderland

Tanaka-Ueguchi M, Itoh H, Oyama N, Koshioka M, Matsuoka M (1998) Over-expression of tobacco homeobox gene, *NTH15*, decreases the expression of a gibberellin biosynthetic gene encoding GA 20-oxidase. Plant J 15:391–400

Thomas SG, Phillips AL, Heddem P (1999) Molecular cloning and functional expression of gibberellin 2-oxidases, multifunctional enzymes involved in gibberellin deactivation. Proc Natl Acad Sci USA 96:4698–4703

Tononi P, Möller M, Bencivenga S, Spada A (2010) *GRAMINIFOLIA* homolog expression in *Streptocarpus rexii* is associated with the basal meristems in phyllomorphs, a morphological novelty in Gesneriaceae. Evol Dev 12:61–73

Veit B (2004) Determination of cell fate in apical meristems. Curr Opin Plant Biol 7:57–64

Wang H, Caruso LV, Downie AB, Perry SE (2004) The embryo MADS domain protein AGAMOUS-like 15 directly regulates expression of a gene encoding an enzyme involved in gibberellin metabolism. Plant Cell 16:1206–1219

Xu Y-L, Li L, Wu K, Peeters AJM, Gage DA, Zeevaart JAD (1995) The *GA5* locus of *Arabidopsis thaliana* encodes a multifunctional gibberellin 20-oxidase: molecular cloning and functional expression. Proc Natl Acad Sci USA 92:6640–6644

Yamaguchi S (2008) Gibberellin metabolism and its regulation. Annu Rev Plant Biol 59:225–251